

Electrical circuits described by a fractional derivative with regular Kernel

J.F. Gómez-Aguilar^{a*}, T. Córdova-Fraga^b, J.E. Escalante-Martínez^c, C. Calderón-Ramón^c, and R.F. Escobar-Jiménez^d

^{a*}*Catedrático del Consejo Nacional de Ciencia y Tecnología-Centro Nacional de Investigación y Desarrollo Tecnológico, Tecnológico Nacional de México.*

Interior Internado Palmira S/N, Col. Palmira, 62490, Cuernavaca, Morelos, México.

^b*Departamento de Ingeniería Física, División de Ciencias e Ingenierías Campus León, Universidad de Guanajuato, León, Guanajuato, México.*

^c*Facultad de Ingeniería Mecánica y Eléctrica, Universidad Veracruzana.*

Av. Venustiano Carranza S/N, Col. Revolución, 93390, Poza Rica Veracruz, México.

^d*Centro Nacional de Investigación y Desarrollo Tecnológico Tecnológico Nacional de México, Interior Internado Palmira S/N, Col. Palmira, C.P. 62490, Cuernavaca, Morelos, México.*

**e-mail: jgomez@cenidet.edu.mx*

Received 3 August 2015; accepted 10 December 2015

In this paper we presented the electrical circuits LC, RC, RL and RLC using a novel fractional derivative with regular kernel called Caputo-Fabrizio fractional derivative. The fractional equations in the time domain considers derivatives of order $(0; 1]$, the analysis is performed in the frequency domain and the conversion in the time domain is performed using the numerical inverse Laplace transform algorithm; furthermore, analytical solutions are presented for these circuits considering different source terms introduced in the fractional equation. The numerical results for different values of the fractional order γ exhibits fluctuations or fractality of time in different scales and the existence of heterogeneities in the electrical components causing irreversible dissipative effects. The classical behaviors are recovered when the order of the temporal derivative is equal to 1 and the system exhibit the Markovian nature.

Keywords: Electrical circuits; Caputo-Fabrizio fractional derivative; fractional-order circuits; oscillations.

PACS: 84.30.Bv; 84.32.Ff; 84.32.Tt

1. Introduction

Classical electrical circuits consist of resistors, inductors and capacitors. However, these electrical components have a non-conservative feature that involve irreversible dissipative effects such as ohmic friction or internal friction, thermal memory and nonlinearities due to the effects of the electric and magnetic fields, these dissipative effects are not considered in the standard theoretical calculations [1-3]. These dissipative effects originate non-conservative systems and equations to describe the behavior of these systems must be non-local differential equations in time; with this purpose, in the last decades the Fractional Calculus (FC) allows the investigation of the nonlocal response of multiple phenomena [4-10], the fractional derivatives are memory operators which usually represent dissipative effects or damage. FC considers the history and non-local distributed effects of any physical system, particularly in electrical circuits, the use of fractional order operators allows us to generalize the propagation of electrical signals in devices, circuits and networks [11-20], as well, the modeling of electrical components (capacitors, coils, memristors, domino ladders, tree structures), see [16-24]. In this context, Rousan in Ref. [25] has suggested a fractional differential equation that combines the simple harmonic oscillations of a LC circuit with the discharging of a RC circuit. In Ref. [20] the simple current

source-wire circuit has been studied fractionally using direct and alternating current source. It was shown that the wire acquires an inducting behavior as the current is initiated in it and gradually recovers its resisting behavior, recently, the authors of [22] considered theoretically and experimentally the charging and discharging processes of different capacitors in electrical RC circuits, the measured experimental results could be exactly obtained within the fractional calculus approach.

Some fundamental definitions in the context of FC are Erdelyi-Kober, Riesz, Riemann-Liouville, Hadamard, Grünwald-Letnikov, Weyl, Jumarie, Caputo [26]- [31]. Some advantages and disadvantages of these fractional derivatives are reviewed by Abdon in [27]. The Riemann-Liouville definition entails physically unacceptable initial conditions (fractional order initial conditions) [28]; conversely for the Caputo representation, the initial conditions are expressed in terms of integer-order derivatives having direct physical significance [29], these definitions have the disadvantage that their kernel present singularity, this kernel include memory effects and therefore both definitions cannot accurately describe the full effect of the memory [32]. Due to this inconvenience, Michele Caputo and Mauro Fabrizio in [33] present a new definition of fractional derivative without singular kernel, the Caputo-Fabrizio (CF) fractional derivative, this derivative possesses very interesting properties, for instance, the pos-

sibility to describe fluctuations and structures with different scales. Furthermore, this definition allows for the description of mechanical properties related with damage, fatigue, material heterogeneities and structures at different scales. Properties of this new fractional derivative are reviewed in detail in Lozada and Nieto [34]. Atangana in Ref. [35] obtained the numerical approximation of the RLC circuit model considering the Caputo-Fabrizio fractional derivative, the author applied the Crank-Nicholson numerical scheme to solve the model proposed. Other applications of the CF fractional derivative are given in Refs. [36-38].

The Numerical Laplace Transform (NLT) is essentially a modified discrete Fourier transform through a windowing function [39]. Development of the NLT and its application to the analysis of systems has been well documented over the past years [40,41]. The use of fast Fourier transform reduces the necessary time for computation and as a result the techniques of analysis in the frequency domain become an attractive option. The results in the frequency domain are then transformed in the time domain by numerical inverse Laplace transform (NILT) algorithm which can be numerically evaluated by the discretized Fourier transform. The truncation of the frequency spectrum can be reduced by the introduction of some suitable data window: Blackman, Hanning, Lanczos or any window function from the literature [41]. In this context, Sheng in Ref. [42] investigated the validity of applying numerical inverse Laplace transform algorithms in FC, the author shows the effectiveness and reliability of applying NILT algorithms for fractional-order differential equations.

In the present work we present the numerical solutions of the electrical circuits LC, RC, RL and RLC using Caputo-Fabrizio fractional derivative for different sources terms, the idea proposed in Ref. [43] is applied in order to preserve the physical dimensionality of the fractional temporal operator.

The manuscript is organized as follows: in Sec. 2, we recall the Caputo-Fabrizio derivative. Section 3 is dedicated to the electrical circuits equations within the Caputo-Fabrizio derivative. Finally, Sec. 4 is devoted to our conclusions.

2. Basic Concepts

The CF definition of fractional derivative is defined as follows [33,34]

$${}_0^{CF} \mathcal{D}_t^\gamma f(t) = \frac{M(\gamma)}{1-\gamma} \int_0^t \dot{f}(\alpha) \exp\left[-\frac{\gamma(t-\alpha)}{1-\gamma}\right] d\alpha, \quad (1)$$

where $d^\gamma/dt^\gamma = {}_0^{CF} \mathcal{D}_t^\gamma$ is a CF derivative with respect to t , $M(\gamma)$ is a normalization function such that $M(0)=M(1)=1$, in this fractional derivative the exponential function helps to reduce the risk of singularity, furthermore, the derivative of a constant is equal to zero and the kernel does not have singularity for $t = \alpha$.

If $n \geq 1$ and $\gamma \in [0, 1]$, the CF fractional derivative, ${}_0^{CF} \mathcal{D}_t^{(\gamma+n)} f(t)$ of order $(n + \gamma)$ is defined by

$${}_0^{CF} \mathcal{D}_t^{(\gamma+n)} f(t) = {}_0^{CF} \mathcal{D}_t^{(\gamma)} ({}_0^{CF} \mathcal{D}_t^{(n)} f(t)). \quad (2)$$

The Laplace transform of (1) is defined as follows [33,34]

$$\begin{aligned} \mathcal{L}[{}_0^{CF} \mathcal{D}_t^{(\gamma+n)} f(t)] &= \frac{1}{1-\gamma} \mathcal{L}\left[f^{(\gamma+n)}(t)\right] \\ &\quad \times \mathcal{L}\left[\exp\left(-\frac{\gamma}{1-\gamma}t\right)\right] \\ &= \frac{s^{n+1} \mathcal{L}[f(t)] - s^n f(0) - s^{n-1} f'(0) \dots - f^{(n)}(0)}{s + \gamma(1-s)}, \quad (3) \end{aligned}$$

for this representation in the time domain is suitable to use the Laplace transform [33,34].

From this expression we have

$$\mathcal{L}[{}_0^{CF} \mathcal{D}_t^\gamma f(t)] = \frac{s \mathcal{L}[f(t)] - f(0)}{s + \gamma(1-s)}, \quad n = 0, \quad (4)$$

$$\begin{aligned} \mathcal{L}[{}_0^{CF} \mathcal{D}_t^{(\gamma+1)} f(t)] &= \frac{s^2 \mathcal{L}[f(t)] - s f(0) - \dot{f}(0)}{s + \gamma(1-s)}, \\ n &= 1. \quad (5) \end{aligned}$$

3. Electrical circuits

According to [43] an auxiliary parameter σ is introduced in order to preserve the physical dimensionality of the fractional temporal operator

$$\begin{aligned} \frac{d}{dt} &\rightarrow \frac{1}{\sigma^{1-\gamma}} \cdot {}_0^{CF} \mathcal{D}_t^\gamma, m, \\ m-1 < \gamma \leq m &\quad m \in M = 1, 2, 3, \dots \quad (6) \end{aligned}$$

and

$$\begin{aligned} \frac{d^2}{dt^2} &\rightarrow \frac{1}{\sigma^{2(1-\gamma)}} \cdot {}_0^{CF} \mathcal{D}_t^{2\gamma}, \\ m-1 < \gamma \leq m, &\quad m \in M = 1, 2, 3, \dots \quad (7) \end{aligned}$$

where γ represents the order of the fractional time derivative and σ must have dimension of seconds. The parameter σ is associated with the temporal components in the system (these components change the time constant of the system and exhibits fractality of time) [21], when $\gamma = 1$ the expressions (6) and (7) are recovered in the traditional sense. From now on, we will apply this idea to generalize the case of the fractional electrical circuits.

3.1. LC electrical circuit

Considering (7), the fractional equation for the electrical circuit LC is given by

$$\frac{L}{\sigma^{2(1-\gamma)}} {}_0^{CF} \mathcal{D}_t^{2\gamma} q(t) + \frac{1}{C} q(t) = V(t), \quad 0 < \gamma \leq 1, \quad (8)$$

where the inductance is L , the capacitance is C and $V(t)$ represents the source. Now we obtain the numerical simulation of Eq. (8) for different source terms.

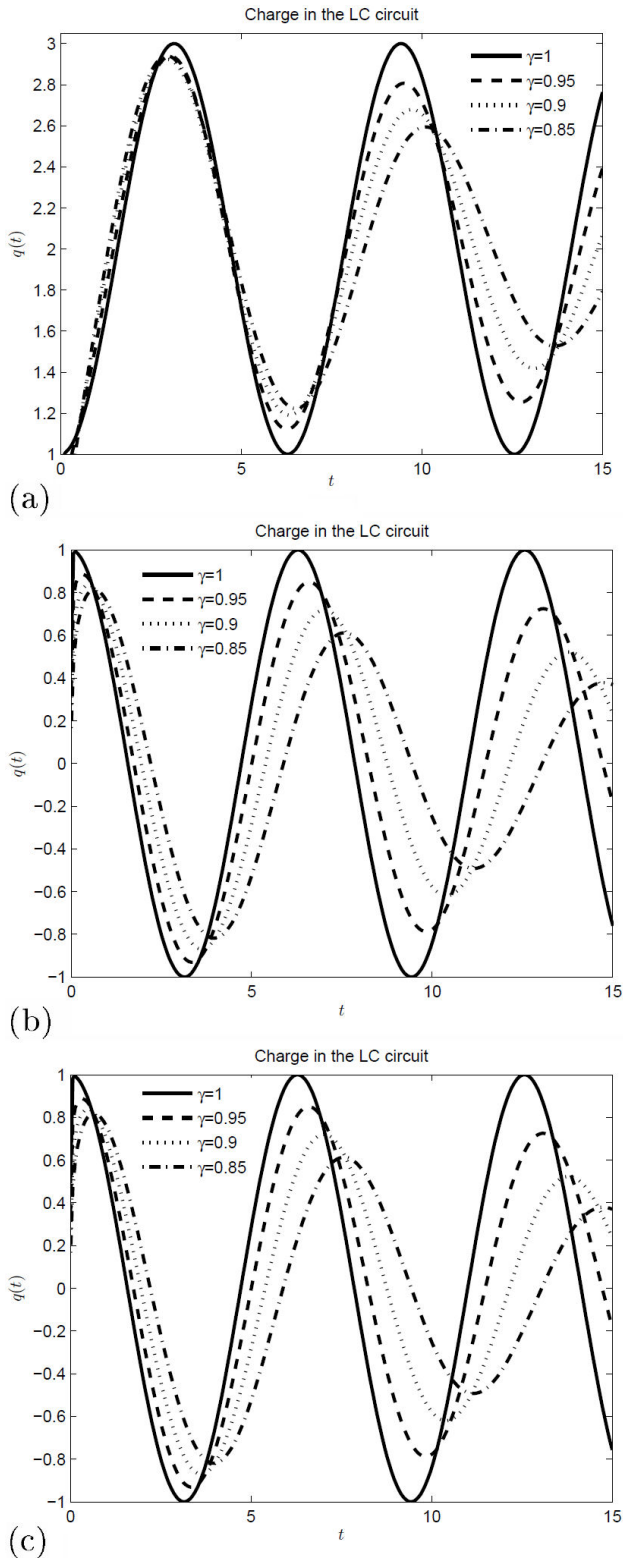


FIGURE 1. LC electrical circuit with different sources.

First Case. Considering the constant source, $V(t) = v_0$, $q(0) = q_0$, ($q_0 > 0$), $\dot{q}(0) = 0$, the Eq. (8) can be written as follows

$${}_0^CF \mathcal{D}_t^{2\gamma} q(t) = \omega^2 C v_0 - \omega^2 q(t), \quad (9)$$

where

$$\omega^2 = \frac{\sigma^{2(1-\gamma)}}{LC} = \omega_0^2 \cdot \sigma^{2(1-\gamma)}, \quad (10)$$

is the fractional angular frequency and $\omega_0 = 1/\sqrt{LC}$ is the natural frequency in the classical case.

Applying the Laplace transform (3) to (9) yields

$$Q(s) = q_0 \cdot \frac{s}{s^2 + \omega^2[s + \gamma(1-s)]} + \omega^2 C v_0 \left(\frac{s + \gamma(1-s)}{s(s^2 + \omega^2[s + \gamma(1-s)])} \right), \quad (11)$$

applying NILT algorithm [42] to (11) we obtain the time response. The plots for different values of the fractional order γ are shown in Fig. (1a).

Second Case. Considering the periodic source, $V(t) = v_0 \cos(\varphi t)$, $q(0) = q_0$, ($q_0 > 0$), $\dot{q}(0) = 0$, the Eq. (8) can be written as follows

$${}_0^CF \mathcal{D}_t^{2\gamma} q(t) = \omega^2 C v_0 \cos(\varphi t) - \omega^2 q(t), \quad (12)$$

where ω^2 is given by (10).

Applying the Laplace transform (3) to (12) yields

$$Q(s) = q_0 \cdot \frac{s}{s^2 + \omega^2[s + \gamma(1-s)]} + \omega^2 C v_0 \left(\frac{s(s + \gamma(1-s))}{(s^2 + \varphi^2)(s^2 + \omega^2[s + \gamma(1-s)])} \right), \quad (13)$$

applying NILT algorithm [42] to (13) we obtain the time response. The plots for different values of the fractional order γ are shown in Fig. (1b).

Third Case. Considering the periodic source, $V(t) = v_0 \sin(\varphi t)$, $q(0) = q_0$, ($q_0 > 0$), $\dot{q}(0) = 0$, the Eq. (8) can be written as follows

$${}_0^CF \mathcal{D}_t^{2\gamma} q(t) = \omega^2 C v_0 \sin(\varphi t) - \omega^2 q(t), \quad (14)$$

where ω^2 is given by (10).

Applying the Laplace transform (3) to (14) yields

$$Q(s) = q_0 \cdot \frac{s}{s^2 + \omega^2[s + \gamma(1-s)]} + \omega^2 C v_0 \left(\frac{\varphi(s + \gamma(1-s))}{(s^2 + \varphi^2)(s^2 + \omega^2[s + \gamma(1-s)])} \right), \quad (15)$$

applying NILT algorithm [42] to (15) we obtain the time response. The plots for different values of the fractional order γ are shown in Fig. (1c).

Now, we obtain the analytical solutions for the fractional Eq. (8), two sources are considered $V(t) = 0$ and $V(t) = v_0 \cdot u(t)$.

First Case. Considering, $V(t) = 0$, $q(0) = q_0$, ($q_0 > 0$), $\dot{q}(0) = 0$, Eq. (8) can be written as follows

$${}_0^CF \mathcal{D}_t^{2\gamma} q(t) = \omega^2 C v_0 - \omega^2 q(t), \quad (16)$$

where ω^2 is given by (10).

Applying the Laplace transform (3) to (21) yields

$$\mathcal{L}\left\{ {}_0^{CF}D_t^{2\alpha}q(t) \right\} = \mathcal{L}\left\{ -w^2q(t) \right\}, \quad (17)$$

due to the linearity of the Laplace transform we have

$$\frac{s(s\tilde{q}(s) - q_0)}{(s + \alpha(1 - s))^2} = -w^2\tilde{q}(s), \quad (18)$$

applying inverse Laplace transform to the above equation yields

$$q(t) = \mathcal{L}^{-1}\left\{ \frac{sq_0}{s^2 + w^2(s + \alpha(1 - s))^2} \right\}, \quad (19)$$

finally, the analytical solution is given by

$$q(t) = q_0 \frac{e^{-i+w(-1+\alpha)t}(i+w(-1+\alpha)) + e^{i+w(-1+\alpha)t}(i+w-w\alpha)}{2(1+iw(-1+\alpha))(i+w(-1+\alpha))}. \quad (20)$$

Second Case. Considering, $V(t) = v_0$, $q(0) = q_0$, ($q_0 > 0$), $\dot{q}(0) = 0$, Eq. (8) can be written as follows

$${}_0^{CF}\mathcal{D}_t^{2\gamma}q(t) = \omega^2 C v_0 - \omega^2 q(t), \quad (21)$$

where ω^2 is given by (10).

Applying the Laplace transform (3) to (21) yields

$$\mathcal{L}\left\{ {}_0^{CF}D_t^{2\alpha}q(t) \right\} = \mathcal{L}\left\{ w^2 C v_0 - w^2 q(t) \right\}, \quad (22)$$

due to the linearity of the Laplace transform we have

$$\frac{s(s\tilde{q}(s) - q_0)}{(s + \alpha(1 - s))^2} = w^2 C v_0 \frac{1}{s} - w^2\tilde{q}(s), \quad (23)$$

applying inverse Laplace transform in the above equation yields

$$q(t) = \mathcal{L}^{-1}\left\{ \frac{w^2 C v_0 (s + \alpha(1 - s))^2 \frac{1}{s}}{s^2 + w^2(s + \alpha(1 - s))^2} \right\} + \mathcal{L}^{-1}\left\{ \frac{sq_0}{s^2 + w^2(s + \alpha(1 - s))^2} \right\}, \quad (24)$$

finally, the analytical solution is given by

$$q(t) = -w^2 C v_0 \left[\frac{ie^{-i-w+w\alpha t} + ie^{\frac{w\alpha}{i-w+w\alpha}t} - we^{\frac{w\alpha}{-i-w+w\alpha}t} + wie^{\frac{w\alpha}{i-w+w\alpha}t}}{2w^2(-1-iw+iw\alpha)(-i-w+w\alpha)} + \frac{w\alpha e^{\frac{w\alpha}{-i-w+w\alpha}t} - w\alpha e^{\frac{w\alpha}{i-w+w\alpha}t}}{2w^2(-1-iw+iw\alpha)(-i-w+w\alpha)} \cdot \frac{1}{w^2} \right] + q_0 \frac{e^{-i+w(-1+\alpha)t}(i+w(-1+\alpha)) + e^{i+w(-1+\alpha)t}(i+w-w\alpha)}{2(1+iw(-1+\alpha))(i+w(-1+\alpha))}. \quad (25)$$

3.2. RC electrical circuit

Considering (6), the fractional equation for the electrical circuit RC is given by

$$\frac{R}{\sigma^{1-\gamma}} {}_0^{CF}\mathcal{D}_t^\gamma q(t) + \frac{1}{C}q(t) = V(t), \quad 0 < \gamma \leq 1, \quad (26)$$

where the resistance is R , the capacitance is C and $V(t)$ represents the source. Now we obtain the numerical simulation of Eq. (26) for different source terms.

First Case. Considering the constant source, $V(t) = v_0$, $q(0) = q_0$, ($q_0 > 0$), Eq. (26) can be written as follows

$${}_0^{CF}\mathcal{D}_t^\gamma q(t) = \tau C v_0 - \tau q(t), \quad (27)$$

where

$$\tau = \frac{\sigma^{1-\gamma}}{RC} = \tau_0 \cdot \sigma^{1-\gamma}, \quad (28)$$

τ is the fractional time constant and $\tau_0 = 1/RC$ is the time constant in the classical case.

Applying the Laplace transform (3) to (27) yields

$$Q(s) = q_0 \cdot \frac{1}{s + \tau[s + \gamma(1 - s)]} + \tau C v_0 \left(\frac{s + \gamma(1 - s)}{s(s + \tau[s + \gamma(1 - s)])} \right), \quad (29)$$

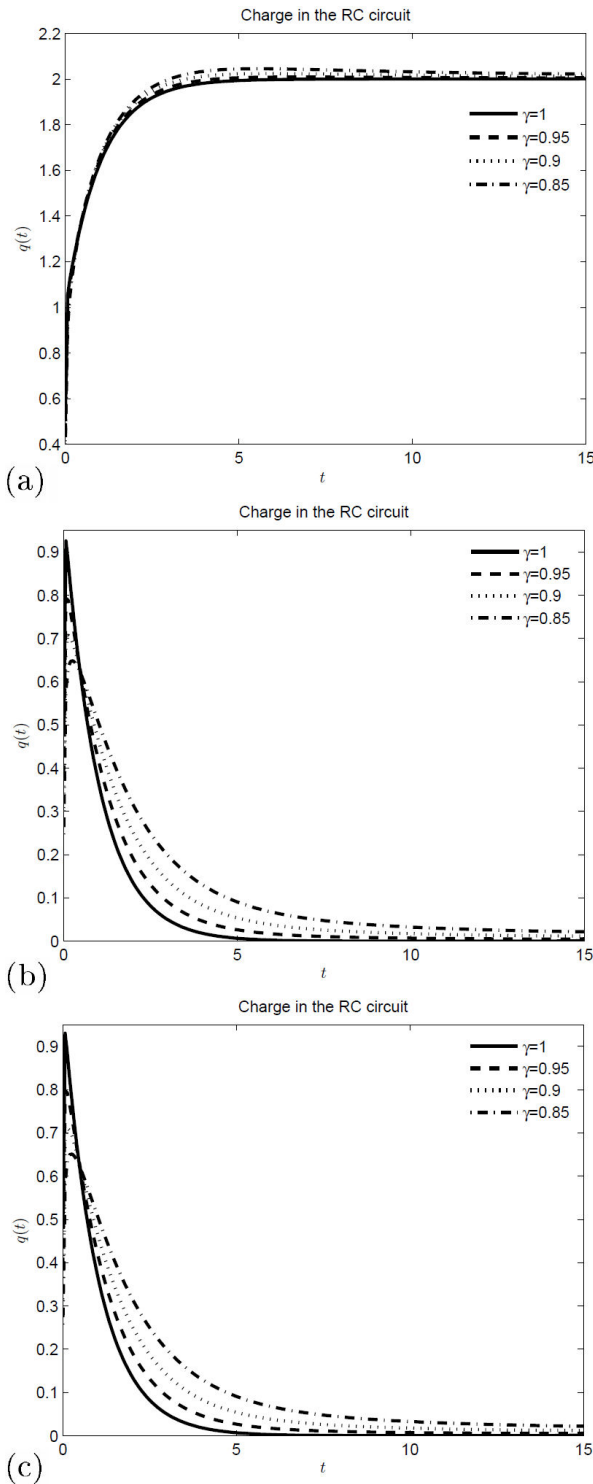


FIGURE 2. RC electrical circuit with different sources.

applying NILT algorithm [42] to (29) we obtain the time response. The plots for different values of the fractional order γ are shown in Fig. (2a).

Second Case. Considering the periodic source, $V(t) = v_0 \cos(\varphi t)$, $q(0) = q_0$, ($q_0 > 0$), Eq. (26) can be written as follows

$${}_0^{CF} \mathcal{D}_t^\gamma q(t) = \tau C v_0 \cos(\varphi t) - \tau q(t), \quad (30)$$

where τ is given by (28).

Applying the Laplace transform (3) to (30) yields

$$Q(s) = q_0 \cdot \frac{1}{s + \tau[s + \gamma(1 - s)]} + \tau C v_0 \left(\frac{s(s + \gamma(1 - s))}{(s^2 + \varphi^2)(s + \tau[s + \gamma(1 - s)])} \right), \quad (31)$$

applying NILT algorithm [42] to (31) we obtain the time response. The plots for different values of the fractional order γ are shown in Fig. (2b).

Third Case. Considering the periodic source, $V(t) = v_0 \sin(\varphi t)$, $q(0) = q_0$, ($q_0 > 0$), Eq. (26) can be written as follows

$${}_0^{CF} \mathcal{D}_t^\gamma q(t) = \tau C v_0 \sin(\varphi t) - \tau q(t), \quad (32)$$

where τ is given by (28).

Applying the Laplace transform (3) to (32) yields

$$Q(s) = q_0 \cdot \frac{1}{s + \tau[s + \gamma(1 - s)]} + \tau C v_0 \left(\frac{\varphi(s + \gamma(1 - s))}{(s^2 + \varphi^2)(s + \tau[s + \gamma(1 - s)])} \right), \quad (33)$$

applying NILT algorithm [42] to (33) we obtain the time response. The plots for different values of the fractional order γ are shown in Fig. (2c).

Considering (6), the fractional equation for the voltage across the capacitor is given by

$$\frac{1}{\sigma^{1-\gamma}} {}_0^{CF} \mathcal{D}_t^\gamma V_c(t) + \frac{1}{RC} V_c(t) = V(t), \quad 0 < \gamma \leq 1, \quad (34)$$

where R is the resistance and C is the capacitance.

First Case. Considering, $V(t) = 0$, $V_c(0) = V_0$, ($V_0 > 0$), Eq. (34) can be written as follows

$${}_0^{CF} \mathcal{D}_t^\gamma V_c(t) + \tau V_c(t) = 0, \quad 0 < \gamma \leq 1, \quad (35)$$

where τ is given by (28).

In this case, the analytical solution is given by

$$V_c(t) = V_0 \exp\left(-\frac{\tau\gamma}{1 + \tau(1 - \gamma)} t\right), \quad 0 < \gamma \leq 1. \quad (36)$$

Second Case. Considering the constant source, $V(t) = v_0$, $V_c(0) = V_0$, ($V_0 > 0$), Eq. (34) can be written as follows

$${}_0^{CF} \mathcal{D}_t^\gamma V_c(t) + \tau V_c(t) = \tau R v_0, \quad 0 < \gamma \leq 1, \quad (37)$$

where τ is given by (28).

In this case, the analytical solution is given by

$$V_c(t) = R v_0 + [V_0 - R v_0] \exp\left(-\frac{\tau\gamma}{1 - \tau(\gamma - 1)} t\right). \quad (38)$$

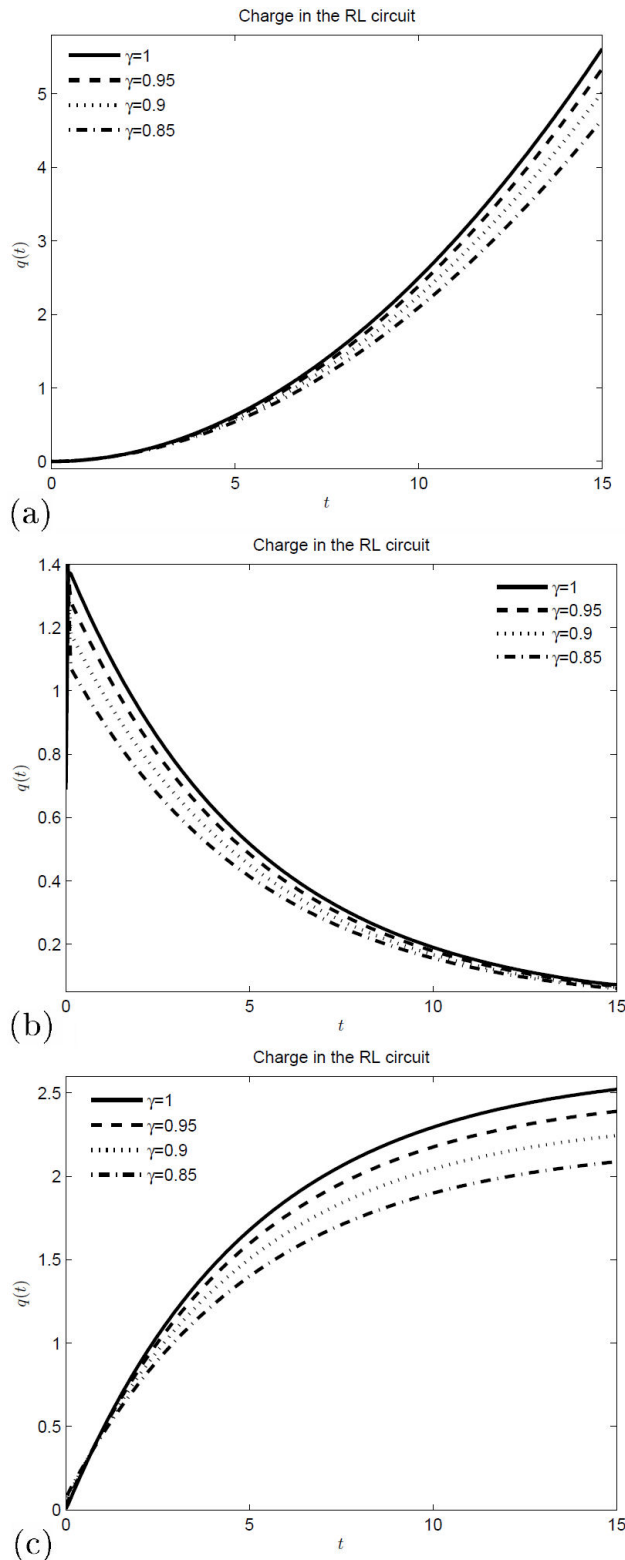


FIGURE 3. RL electrical circuit with different sources.

3.3. RL electrical circuit

Considering (6) and (7), the fractional equation for the electrical circuit RL is given by

$$\frac{L}{\sigma^{2(1-\gamma)}} {}_0^{CF} \mathcal{D}_t^{2\gamma} q(t) + \frac{R}{\sigma^{1-\gamma}} {}_0^{CF} \mathcal{D}_t^\gamma q(t) = V(t), \quad 0 < \gamma \leq 1, \quad (39)$$

where the inductance is L , the resistance is R and $V(t)$ represents the source. Now we obtain the numerical simulation of Eq. (39) for different source terms.

First Case. Considering the constant source, $V(t) = v_0$, $q(0) = q_0$, ($q_0 > 0$), $\dot{q}(0) = 0$, Eq. (39) can be written as follows

$${}_0^{CF} \mathcal{D}_t^{2\gamma} q(t) + A \cdot {}_0^{CF} \mathcal{D}_t^\gamma q(t) = Bv_0, \quad (40)$$

where

$$A = \frac{R}{L} \sigma^{1-\gamma}, \quad (41)$$

and

$$B = \frac{1}{L} \sigma^{2(1-\gamma)}. \quad (42)$$

Applying the Laplace transform (3) to (40) yields

$$Q(s) = q_0 \left(\frac{s + A}{s^2 + As} \right) + Bv_0 \left(\frac{s + \gamma(1-s)}{s(s^2 + As)} \right), \quad (43)$$

applying NILT algorithm [42] to (43) we obtain the time response. The plots for different values of the fractional order γ are shown in Fig. (3a).

Second Case. Considering the periodic source, $V(t) = v_0 \cos(\varphi t)$, $q(0) = q_0$, ($q_0 > 0$), $\dot{q}(0) = 0$, Eq. (39) can be written as follows

$${}_0^{CF} \mathcal{D}_t^{2\gamma} q(t) + A \cdot {}_0^{CF} \mathcal{D}_t^\gamma q(t) = Bv_0 \cos(\varphi t), \quad (44)$$

where A and B are given by (41) and (42).

Applying the Laplace transform (3) to (44) yields

$$Q(s) = q_0 \left(\frac{s + A}{s^2 + As} \right) + Bv_0 \left(\frac{s(s + \gamma(1-s))}{(s^2 + As)(s^2 + \varphi^2)} \right), \quad (45)$$

applying NILT algorithm [42] to (45) we obtain the time response. The plots for different values of the fractional order γ are shown in Fig. (3b).

Third Case. Considering the periodic source, $V(t) = v_0 \sin(\varphi t)$, $q(0) = q_0$, ($q_0 > 0$), $\dot{q}(0) = 0$, Eq. (39) can be written as follows

$${}_0^{CF} \mathcal{D}_t^{2\gamma} q(t) + A \cdot {}_0^{CF} \mathcal{D}_t^\gamma q(t) = Bv_0 \sin(\varphi t), \quad (46)$$

where A and B are given by (41) and (42).

Applying the Laplace transform (3) to (46) yields

$$Q(s) = q_0 \left(\frac{s + A}{s^2 + As} \right) + Bv_0 \left(\frac{\varphi(s + \gamma(1-s))}{(s^2 + As)(s^2 + \varphi^2)} \right), \quad (47)$$

applying NILT algorithm [42] to (47) we obtain the time response. The plots for different values of the fractional order γ are shown in Fig. (3c).

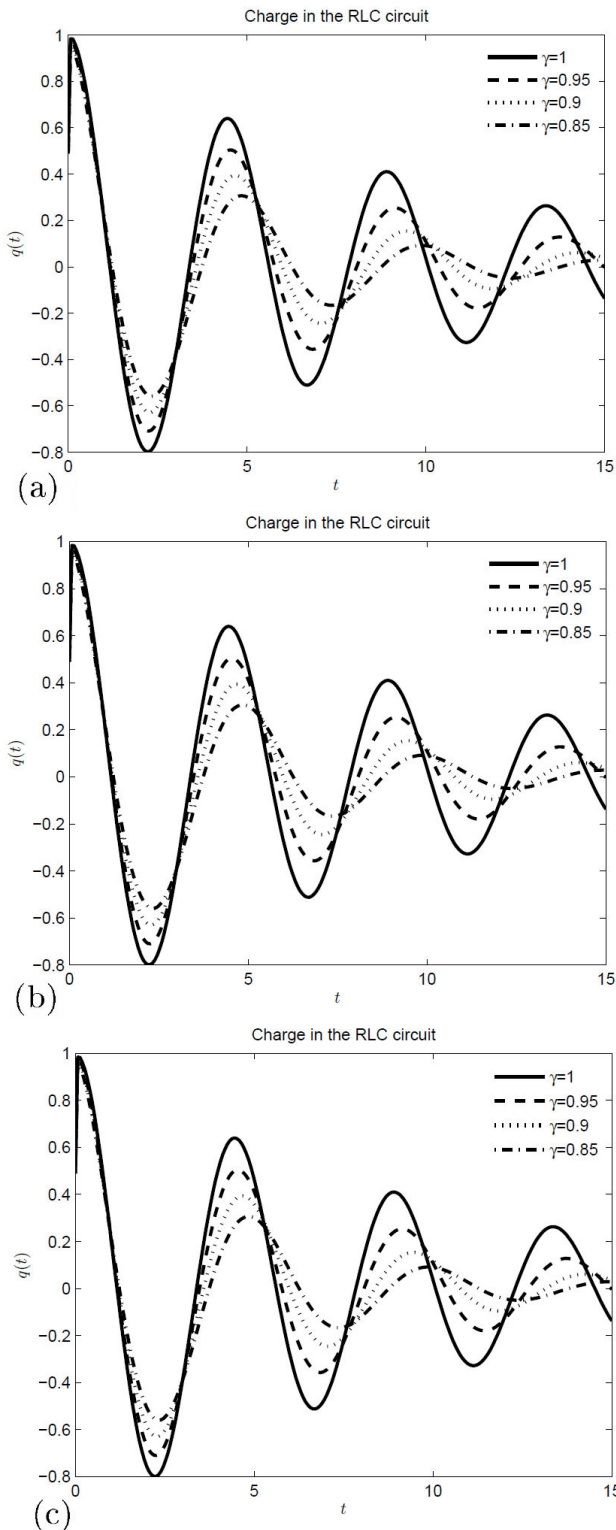


FIGURE 4. RLC electrical circuit with different sources.

Considering (6), the fractional equation for the current across the inductor is given by

$$\frac{L}{\sigma^{1-\gamma}} {}_0^CF \mathcal{D}_t^\gamma I(t) + RI(t) = V(t), \quad 0 < \gamma \leq 1, \quad (48)$$

where L is the inductance and R is the resistance.

First Case. Considering, $V(t) = 0, I(0) = I_0, (I_0 > 0)$, Eq. (48) can be written as follows

$${}_0^CF \mathcal{D}_t^\gamma I(t) + \eta I(t) = 0, \quad 0 < \gamma \leq 1, \quad (49)$$

where

$$\eta = \frac{\sigma^{1-\gamma}}{\eta_0}, \quad (50)$$

η is the fractional time constant and $\eta_0 = L/R$ is the time constant in the classical case.

In this case, the analytical solution is given by

$$I(t) = I_0 \exp\left(-\frac{\eta\gamma}{1-\eta(\gamma-1)}t\right), \quad 0 < \gamma \leq 1. \quad (51)$$

Second Case. Considering the constant source, $V(t) = v_0, I(0) = I_0, (I_0 > 0)$, Eq. (48) can be written as follows

$${}_0^CF \mathcal{D}_t^\gamma I(t) + \eta I(t) = \frac{\eta}{R}v_0, \quad 0 < \gamma \leq 1, \quad (52)$$

where η is given by (50).

In this case, the analytical solution is given by

$$I(t) = \frac{v_0}{R} + \left[I_0 - \frac{v_0}{R}\right] \exp\left(-\frac{\eta\gamma}{1-\eta(\gamma-1)}t\right). \quad (53)$$

3.4. RLC electrical circuit

Considering (6) and (7), the fractional equation for the electrical circuit RLC is given by

$$\frac{L}{\sigma^{2(1-\gamma)}} {}_0^CF \mathcal{D}_t^{2\gamma} q(t) + \frac{R}{\sigma^{1-\gamma}} {}_0^CF \mathcal{D}_t^\gamma q(t) + \frac{1}{C}q(t) = V(t), \quad 0 < \gamma \leq 1, \quad (54)$$

where the inductance is L , the resistance is R , the capacitance is C and $V(t)$ represents the source. Now we obtain the numerical simulation of Eq. (54) for different source terms.

First Case. Considering the constant source, $V(t) = v_0, q(0) = q_0, (q_0 > 0), \dot{q}(0) = 0$, Eq. (54) can be written as follows

$${}_0^CF \mathcal{D}_t^{2\gamma} q(t) + A \cdot {}_0^CF \mathcal{D}_t^\gamma q(t) + Dq(t) = Bv_0, \quad (55)$$

where A and B are given by (41), (42), respectively and

$$D = \frac{1}{LC}\sigma^{2(1-\gamma)}. \quad (56)$$

Applying the Laplace transform (3) to (62) yields

$$Q(s) = q_0 \left(\frac{s + A}{s^2 + As + D(s + \gamma(1-s))} \right) + Bv_0 \left(\frac{s + \gamma(1-s)}{s[s^2 + As + D(s + \gamma(1-s))]} \right), \quad (57)$$

applying NILT algorithm [42] to (57) we obtain the time response. The plots for different values of the fractional order γ are shown in Fig. (4a).

Second Case. Considering the periodic source, $V(t) = v_0 \cos(\varphi t)$, $q(0) = q_0$, ($q_0 > 0$), $\dot{q}(0) = 0$, Eq. (54) can be written as follows

$${}_0^{CF} \mathcal{D}_t^{2\gamma} q(t) + A \cdot {}_0^{CF} \mathcal{D}_t^\gamma q(t) + Dq(t) = Bv_0 \cos(\varphi t), \quad (58)$$

where A, B and D are given by (41), (42) and (56), respectively.

Applying the Laplace transform (3) to (58) yields

$$Q(s) = q_0 \left(\frac{s + A}{s^2 + As + D(s + \gamma(1 - s))} \right) + Bv_0 \left(\frac{s(s + \gamma(1 - s))}{(s^2 + \varphi^2)[s^2 + As + D(s + \gamma(1 - s))]} \right), \quad (59)$$

applying NILT algorithm [42] to (59) we obtain the time response. The plots for different values of the fractional order γ are shown in Fig. (4b).

Third Case. Considering the periodic source, $V(t) = v_0 \sin(\varphi t)$, $q(0) = q_0$, ($q_0 > 0$), $\dot{q}(0) = 0$, Eq. (54) can be written as follows

$${}_0^{CF} \mathcal{D}_t^{2\gamma} q(t) + A \cdot {}_0^{CF} \mathcal{D}_t^\gamma q(t) + Dq(t) = Bv_0 \sin(\varphi t), \quad (60)$$

where A, B and D are given by (41), (42) and (56), respectively.

Applying the Laplace transform (3) to (60) yields

$$Q(s) = q_0 \left(\frac{s + A}{s^2 + As + D(s + \gamma(1 - s))} \right) + Bv_0 \left(\frac{\varphi(s + \gamma(1 - s))}{(s^2 + \varphi^2)[s^2 + As + D(s + \gamma(1 - s))]} \right), \quad (61)$$

applying NILT algorithm [42] to (61) we obtain the time response. The plots for different values of the fractional order γ are shown in Fig. (4c).

First Case. Considering, $V(t) = 0$, $q(0) = q_0$, ($q_0 > 0$), $\dot{q}(0) = 0$, Eq. (54) can be written as follows

$${}_0^{CF} \mathcal{D}_t^{2\gamma} q(t) + A \cdot {}_0^{CF} \mathcal{D}_t^\gamma q(t) + Dq(t) = 0, \quad (62)$$

where A and D are given by (41) and (56), respectively.

Applying the Laplace transform to (62) yields

$$\mathcal{L} \left\{ {}_0^{CF} D_t^{2\gamma} q(t) + A {}_0^{CF} D_t^\gamma q(t) = -Dq(t) \right\}$$

considering (3) and the ordinary Laplace transform we have

$$\frac{s(\tilde{q}(s) - q_0)}{(s + \gamma(1 - s))^2} + \frac{A(\tilde{q}(s) - q_0)}{(s + \gamma(1 - s))} = -D\tilde{q}(s), \quad (63)$$

the charge $\tilde{q}(s)$ is given by

$$\tilde{q}(s) = \frac{sq_0}{[s^2 + As(s + \gamma(1 - s)) + D(s + \gamma(1 - s)^2)]} + \frac{Aq_0(s + \gamma(1 - s))}{[s^2 + As(s + \gamma(1 - s)) + D(s + \gamma(1 - s)^2)]}. \quad (64)$$

Applying the inverse Laplace transform to (64) we have

$$q(t) = \left(\exp \left(\frac{t + (A + \sqrt{A^2 - 4D} - 2D(\gamma - 1))\gamma}{2(1 + A + D(\gamma - 1)^2) - A\gamma} \right) \cdot q_0 \left(-\sqrt{A^2 - 4D} \left(1 + \exp \left(\frac{\sqrt{A^2 - 4D}t\gamma}{1 + A + D(\gamma - 1)^2 - A\gamma} \right) \right) \right) + A^2 \left(-1 + \exp \left(\frac{\sqrt{A^2 - 4D}t\gamma}{1 + A + D(\gamma - 1)^2 - A\gamma} \right) \right) (\gamma - 1) - 2D \left(-1 + \exp \left(\frac{\sqrt{A^2 - 4D}t\gamma}{1 + A + D(\gamma - 1)^2 - A\gamma} \right) \right) (\gamma - 1) + A \left(1 - \sqrt{A^2 - 4D} + \sqrt{A^2 - 4D}\gamma + \exp \left(\frac{\sqrt{A^2 - 4D}t\gamma}{1 + A + D(\gamma - 1)^2 - A\gamma} \right) \times \left(-1 - \sqrt{A^2 - 4D} + \sqrt{A^2 - 4D} \right) \right) \right) 2\sqrt{A^2 - 4D} \left(-1 + A(\gamma - 1) - D(\gamma - 1)^2 \right), \quad 0 < \gamma \leq 1. \quad (65)$$

The inverse Laplace transform can be easily solved, especially by means of symbolic computation software such as Mathematica, Maple, Matlab, etc.

Second Case. Considering, $V(t) = v_0$, $q(0) = q_0$, ($q_0 > 0$), $\dot{q}(0) = 0$, Eq. (54) can be written as follows

$${}_0^{CF} \mathcal{D}_t^{2\gamma} q(t) + A \cdot {}_0^{CF} \mathcal{D}_t^\gamma q(t) + Dq(t) = Bv_0 - Dq(t), \quad (66)$$

where A and D are given by (41) and (56), respectively.

Applying the Laplace transform to (66) yields

$$\mathcal{L} \left\{ {}_0^{CF} D_t^{2\gamma} q(t) + A {}_0^{CF} D_t^\gamma q(t) = Bv_0 - Dq(t) \right\}$$

considering (3) and the ordinary Laplace transform we have

$$\frac{s(s\tilde{q}(s) - q_0)}{(s + \gamma(1 - s))^2} + \frac{A(s\tilde{q}(s) - q_0)}{(s + \gamma(1 - s))} = B\frac{v_0}{s} - D\tilde{q}(s). \tag{67}$$

the charge $\tilde{q}(s)$ is given by

$$\begin{aligned} \tilde{q}(s) &= \frac{B(s + \gamma(1 - s))^2}{[s^2 + As(s + \gamma(1 - s)) + D(s + \gamma(1 - s)^2)]} \cdot \frac{v_0}{s} \\ &+ \frac{sq_0}{[s^2 + As(s + \gamma(1 - s)) + D(s + \gamma(1 - s)^2)]} + \frac{Aq_0(s + \gamma(1 - s))}{[s^2 + As(s + \gamma(1 - s)) + D(s + \gamma(1 - s)^2)]}. \end{aligned} \tag{68}$$

Applying the inverse Laplace transform to (68) we have

$$\begin{aligned} q(t) &= \left(\frac{1}{2\sqrt{A^2 - 4D}D^2\gamma} B \exp\left(\frac{-t(A + \sqrt{A^2 - 4D} - 2D(\gamma - 1))\gamma}{2(1 + A + D(\gamma - 1)^2 - A\gamma)}\right) \right) \cdot v_0 \\ &\cdot \left[A^2 \left(-1 + \exp\left(\frac{\sqrt{A^2 - 4D}t\gamma}{1 + A + D(\gamma - 1)^2 - A\gamma}\right) \right) + A\sqrt{A^2 - 4D} \left(1 + \exp\left(\frac{\sqrt{A^2 - 4D}t\gamma}{1 + A + D(\gamma - 1)^2 - A\gamma}\right) \right) \right. \\ &- 2 \exp\left(\frac{t(A + \sqrt{A^2 - 4D} - 2D(\gamma - 1))\gamma}{2(1 + A + D(\gamma - 1)^2 - A\gamma)}\right) - 2D \left(-1 + \exp\left(\frac{\sqrt{A^2 - 4D}t\gamma}{1 + A + D(\gamma - 1)^2 - A\gamma}\right) \right) \\ &- \left. \sqrt{A^2 - 4D} \exp\left(\frac{t\gamma(A + \sqrt{A^2 - 4D} - 2D(\gamma - 1))}{2(1 + A + D(\gamma - 1)^2 - A\gamma)}\right) t\gamma \right] + \exp\left(\frac{t + (A + \sqrt{A^2 - 4D} - 2D(\gamma - 1))\gamma}{2(1 + A + D(\gamma - 1)^2 - A\gamma)}\right) \\ &\cdot q_0 \left(-\sqrt{A^2 - 4D} \left(1 + \exp\left(\frac{\sqrt{A^2 - 4D}t\gamma}{1 + A + D(\gamma - 1)^2 - A\gamma}\right) \right) \right) + A^2 \left(-1 + \exp\left(\frac{\sqrt{A^2 - 4D}t\gamma}{1 + A + D(\gamma - 1)^2 - A\gamma}\right) \right) (\gamma - 1) \\ &- 2D \left(-1 + \exp\left(\frac{\sqrt{A^2 - 4D}t\gamma}{1 + A + D(\gamma - 1)^2 - A\gamma}\right) \right) (\gamma - 1) + A \left(1 - \sqrt{A^2 - 4D} + \sqrt{A^2 - 4D}\gamma \right) \\ &\times \exp\left(\frac{\sqrt{A^2 - 4D}t\gamma}{1 + A + D(\gamma - 1)^2 - A\gamma}\right) \left(-1 - \sqrt{A^2 - 4D} + \sqrt{A^2 - 4D}\gamma \right) \Bigg) \Bigg) \Bigg) \Bigg) / 2\sqrt{A^2 - 4D} \\ &\times \left(-1 + A(\gamma - 1) - D(\gamma - 1)^2 \right), \quad 0 < \gamma \leq 1. \end{aligned} \tag{69}$$

The inverse Laplace transform can be easily solved, especially by means of symbolic computation software such as Mathematica, Maple, Matlab, etc.

4. Conclusion

In this work we present an alternative representation of fractional differential equations for the electrical circuits LC, RC, RL and RLC using Caputo-Fabrizio fractional derivative, analytical and numerical solutions were obtained. These fractional representations were obtained preserving the dimensionality of the system studied for any value taken by the exponent of the fractional derivative.

The numerical solutions show a change in the amplitude of the charge and variations in the phase exhibits fractality in time to different scales and shows the existence of heterogeneities in the electrical components (resistance, capaci-

tance and inductance). These behaviors depend on the fractional derivative order and modified the constant time of the electrical circuits, particularly when γ is less than 1, the systems exhibit a fast stabilization (is not as affected by past) than it takes the integer exponent. The Caputo-Fabrizio approach allows to describe the relaxation phenomena and dissipative processes that characterize the electrical circuits, the numerical solution exhibits temporal fractality at different scales as well as the existence of material heterogeneities in the electrical components.

The results gathered in Figs. 1 to 4 briefly show that when $\gamma = 1$, the system displays the Markovian nature. However, for values of $\gamma < 1$, the equations describe non-conservative systems (non-local in time), in this context, the different γ values exhibit fractional time components (such components change the time constant of the system) [21]. At the range

$\gamma \in (0.85, 1)$ the Figures show that the system presents dissipative effects that corresponds to the nonlinear situation of the physical process (realistic behavior that is non-local in time). In these cases the systems modified the damping capacity, for example, when $\gamma = 0.85$ the damping capacity is bigger than when $\gamma = 0.95$. Furthermore, the Figures demonstrate that the Caputo-Fabrizio fractional derivative show a rapid stabilization unlike the definition of Caputo, this definition is affected more by past (memory effect) [17-23].

The resulting equations represent a generalization of the classical electrical circuits LC, RC, RL and RLC, the proposed representation can be used to describe a wide variety of systems which had not been addressed due to the limitations of the classical calculus. In this context, we consider

that these results are useful to understand the behavior of fractional analogical filters, transmission lines, electrical machinery, semiconductors circuits, power electronics, communication theory, equivalent circuits in description of biological and electrochemical systems, control theory, and modeling of cells seen as electrical circuits.

Acknowledgments

We would like to thank to Mayra Martínez for the interesting discussions. We especially thank to Andrea del Rocio Zapata for her final grammar and spelling revision. José Francisco Gómez Aguilar acknowledges the support provided by CONACyT: cátedras CONACyT para jóvenes investigadores 2014.

1. M. de Wild, W. Pomp, G.H. Koenderink, *Biophysical Journal*, **105** (2013) 200-210.
2. Sungho Kim *et al.*, *Physical electro-thermal model of resistive switching in bi-layered resistance-change memory*. Scientific Reports 3, Article number: 1680, doi:10.1038/srep01680.
3. C.H. Henager, W.T. Pawlewicz, *Thermal conductivities of thin, sputtered optical films*. Applied Optics, **32** (1993) 91-101.
4. D. Baleanu, Z.B. Günvenc and J.A. Tenreiro Machado, *New Trends in Nanotechnology and Fractional Calculus Applications*. Springer, (2010).
5. V.E. Tarasov, *Fractional dynamics: applications of fractional calculus to dynamics of particles, fields and media*. Springer Science & Business Media, (2011).
6. J.F. Gómez Aguilar and M. Miranda Hernández, *Space-Time Fractional Diffusion-Advection Equation with Caputo Derivative*. Abstract and Applied Analysis, **2014**, Article ID 283019, 8 pages, (2014). doi:10.1155/2014/283019
7. V. Mishra, K. Vishal, S. Das and S.H. Ong, *Z. Naturforsch* **69a** (2014) 135-144.
8. J.F. Gómez Aguilar, D. Baleanu, *Proceedings of the Romanian Academy, Series A*. **1-15** (2014) 27-34.
9. T.M. Atanackovic, S. Pilipovic, B. Stankovic, D. Zorica, *Fractional Calculus with Applications in Mechanics: Vibrations and Diffusion Processes*. Wiley, London (2014).
10. J.F. Gómez Aguilar and D. Baleanu, *Z. Naturforsch.* **69** (2014) 539-546. Doi:10.5560/ZNA.2014-0049.
11. S. Kumar, *Z. Naturforsch.* **68** (2013) 777-784.
12. H. Samavati, A. Hajimiri, A.R. Shahani, G.N. Nasserbakht, T.H. Lee, *IEEE Journal of Solid-State Circuits* **33** (1998) 2035-2041.
13. S.I. Ravello Arias, D. Ramírez Muñoz, J. Sánchez Moreno, S. Cardoso, R. Ferreira and P.J. Peixeiro de Freitas, *Sensors* **13** (2013) 17516-17533. doi:10.3390/s131217516,.
14. J.F. Gómez Aguilar, *Behavior Characteristic of a Cap-Resistor, Memcapacitor and a Memristor from the Response Obtained of RC and RL Electrical Circuits Described by Fractional Differential Equations*. Turkish Journal of Electrical Engineering & Computer Sciences. Accepted for publication.
15. R. Caponetto, G. Dongola, G. Maione, A. Pisano, *Journal of Vibration and Control*. **20** (2014) 1066-1075.
16. A.S. Elwakil, *Circuits and Systems Magazine, IEEE* **10.4** (2010) 40-50.
17. F. Gómez, J. Rosales, M. Guía, *Cent. Eur. J. Phys.* Springer. (2013).
18. M. Guía, F. Gómez, J. Rosales, *Cent. Eur. J. Phys.* Springer. (2013).
19. F. Gómez-Aguilar, R. Razo-Hernández, J. Rosales-García, M. Guía-Calderón, *Revista de Ingeniería, Investigación y Tecnología, UNAM*. **2** (2014) 311-319.
20. A. Obeidat, M. Gharibeh, M. Al-Ali, A. Rousan, *Fract. Calc. App. Anal* **14**, Springer (2011).
21. J.F. Gómez-Aguilar, R. Razo-Hernández, D. Granados-Lieberman, *Rev. Mex. Fis.* **60** (2014) 32-38.
22. H. Ertik, A.E. Çalik, H. Şirin, M.Şen, B. Öder, *Rev. Mex. Fis.* **61** (2015) 58-63.
23. J. Valsa, J. Vlach, *International Journal of Circuit Theory and Applications* **41** (2013) 59-67.
24. J. Chen, Z. Zeng, P. Jiang, *Neural Networks* **51** (2014) 1-8.
25. A.A. Rousan *et al.*, *Fractional Calculus and Applied analysis*, **9** (2006) 33-41.
26. K.B. Oldham and J. Spanier, *The Fractional Calculus*. Academic Press, New York, (1974).
27. A. Atangana, A. Secer, *Abstract and Applied Analysis* **2013** (2013). Doi:10.1155/2013/279681.
28. K. Diethelm, *The Analysis of Fractional Differential Equations. An Application-Oriented Exposition Using Differential Operators of Caputo Type* (Springer-Verlag, Berlin, Heidelberg, 2010).
29. K. Diethelm, N.J. Ford, A.D. Freed, Yu. Luchko, *Comp. Methods in Appl. Mech. and Eng.* **194** (2005) 743-773.

30. D. Baleanu, K. Diethelm, E. Scalas, J.J. Trujillo, *Fractional Calculus Models and Numerical Methods*. Series on Complexity, Nonlinearity and Chaos. World Scientific, (2012).
31. I. Podlubny, *Fractional Differential Equations*. Academic Press, New York, (1999).
32. A. Atangana, B.S.T. Alkahtani, *Entropy* **17** (2015) 4439-4453.
33. M. Caputo, M. Fabrizio, *Progr. Fract. Differ. Appl.* **1** (2015) 73-85.
34. J. Lozada, J.J. Nieto, *Progr. Fract. Differ. Appl.* **1** (2015) 87-92.
35. A. Atangana, J.J. Nieto, *Advances in Mechanical Engineering*, **7** (2015) 1-6.
36. A. Atangana, B.S.T. Alkahtani, *Advances in Mechanical Engineering*, **7** (2015) 1-6.
37. H. Batarfi, J. Losada, J.J. Nieto, W. Shammakh, *Journal of Function Spaces* (2015).
38. J.F. Gómez-Aguilar *et al.*, *Entropy* **17** (2015) 6289-6303.
39. J.G. Proakis and D.G. Manolakis, *Digital Signal Processing, in Principles, Algorithms and Applications*. 3rd ed. Upper Saddle River, NJ: Prentice-Hall, (1996).
40. D.J. Wilcox, I.S. Gibson, *Int. J. Numer. Methods Eng.* **20** (1984) 1507-1519.
41. P. Moreno, A. Ramírez, *IEEE Trans. Power Delivery.* **23** (2008) 2599-2609.
42. H. Sheng, Y. Li, Y. Chen, *Journal of the Franklin Institute* **348** (2011) 315-330.
43. J.F. Gómez-Aguilar, J.J. Rosales-García, J.J. Bernal-Alvarado, T. Córdova-Fraga, R. Guzmán-Cabrera, *Rev. Mex. Fis* **58** (2012) 524-537.